Analyst

ROYAL SOCIETY OF CHEMISTRY

PAPER

View Article Online
View Journal | View Issue

Cite this: *Analyst*, 2022, **147**, 1159

Differentiating aspartic acid isomers and epimers with charge transfer dissociation mass spectrometry (CTD-MS)

Halle M. Edwards,[a] Hoi-Ting Wu,[b] Ryan R. Julian [b] and Glen P. Jackson *[a,c]

Received 15th December 2021,
Accepted 14th February 2022

DOI: 10.1039/d1an02279b

rsc.li/analyst

The ability to understand the function of a protein often relies on knowledge about its detailed structure. Sometimes, seemingly insignificant changes in the primary structure of a protein, like an amino acid substitution, can completely disrupt a protein's function. Long-lived proteins (LLPs), which can be found in critical areas of the human body, like the brain and eye, are especially susceptible to primary sequence alterations in the form of isomerization and epimerization. Because long-lived proteins do not have the corrective regeneration capabilities of most other proteins, points of isomerism and epimerization that accumulate within the proteins can severely hamper their functions and can lead to serious diseases like Alzheimer's disease, cancer and cataracts. Whereas tandem mass spectrometry (MS/MS) in the form of collision-induced dissociation (CID) generally excels at peptide characterization, MS/MS often struggles to pinpoint modifications within LLPs, especially when the differences are only isomeric or epimeric in nature. One of the most prevalent and difficult-to-identify modifications is that of aspartic acid between its four isomeric forms: L-Asp, L-isoAsp, D-Asp, and D-isoAsp. In this study, peptides containing isomers of Asp were analyzed by charge transfer dissociation (CTD) mass spectrometry to identify spectral features that could discriminate between the different isomers. For the four isomers of Asp in three model peptides, CTD produced diagnostic ions of the form c_n+57 on the N-terminal side of iso-Asp residues, but not on the N-terminal side of Asp residues. Using CTD, the L- and D forms of Asp and isoAsp could also be differentiated based on the relative abundance of *y*- and *z* ions on the C-terminal side of Asp residues. Differentiation was accomplished through a chiral discrimination factor, *R*, which compares an ion ratio in a spectrum of one epimer or isomer to the same ion ratio in the spectrum of a different epimer or isomer. The *R* values obtained using CTD are as robust and statistically significant as other fragmentation techniques, like radical directed dissociation (RDD). In summary, the extent of backbone and side-chain fragments produced by CTD enabled the differentiation of isomers and epimers of Asp in a variety of peptides.

Introduction

Proteins in the human body perform various vital functions to maintain health and homeostasis. Most proteins have relatively short lifetimes, on the order of days or weeks, and are regenerated frequently. However, other proteins—like elastin, collagen, nuclear pores, and eye lens crystalline—have long lifetimes on the order of decades.[1–3] Throughout a protein's lifetime, spontaneous modifications such as oxidation, isomerization and epimerization can occur, and these modifications can accumulate in long-lived proteins that are not regularly replaced.[4] These accumulated modifications can lead to conformational changes in the protein structure, aggregation and loss of function, which can be a root cause of many debilitating diseases that are linked to degeneration.

Alzheimer's is one such neurodegenerative disease that is marked by a loss of synaptic function in the brain and can be linked to aggregations of amyloid beta and tau proteins.[5,6] Similarly, other degenerative diseases—like Parkinson's, Huntington's, cystic fibrosis and certain cancers—likely originate from protein misfolding and subsequent aggregation.[7] Cataracts, which is the leading cause of blindness worldwide, develops due to the breakdown of eye lens crystalline over time and results in an altered protein structure that is less transparent than the properly folded form.[8,9] In addition to the importance in studying degenerative diseases, knowledge of protein

[a]*C. Eugene Bennett Department of Chemistry, West Virginia University, Morgantown, WV, USA. E-mail: glen.jackson@mail.wvu.edu*
[b]*Department of Chemistry, University of California, Riverside, CA, USA*
[c]*Department of Forensic and Investigative Science, West Virginia University, Morgantown, WV, USA*

structure and post translational modifications is important to the development of therapeutic antibodies, especially because loss of function can decrease antigen binding, thereby limiting the effectiveness of treatments.[10,11]

All twenty amino acids that make up proteins within the human body can undergo racemization from the preferred L-form to the D-form, but the rates of racemization vary considerably. For example, aspartic acid racemizes at least four times more quickly than other amino acids.[12] Due to its rapid racemization, L-Asp to D-Asp isomerization has been more widely observed in biological systems and has been more widely studied.[13–15] It is well known that aspartic acid in a protein—whether from translation or from deamidation of asparagine—is prone to forming a stable succinimide ring intermediate following self-nucleophilic attack. Subsequent ring opening and/or stereo-inversion converts aspartate to one of four isomeric forms: L-Asp, D-Asp, L-isoAsp, and D-isoAsp.[16] All four forms of Asp have been detected in the human brain, although L-Asp is the original form produced *via* translation.[17,18] Accumulation of D-Asp is often observed in long-lived proteins, and D-Asp is linked to age related diseases like cataracts.[19–21] Additionally, D-Asp is found at higher concentrations than L-Asp in the brains of Alzheimer's patients.[22] In fact, the link between aging and racemization is so well formed that measurements of D-enantiomers can be used as a tool to estimate the age of biological material in forensic and archaeologic applications.[14,23]

Many different mass spectrometry methods have attempted to differentiate the four forms of Asp, with varying degrees of success.[24,25] Although they are isomeric, the structural differences between Asp and isoAsp are distinguishable because they can produce some unique fragment ions or fragment ions with different relative abundances. Commonly observed b_n+H_2O and y_n-46 ions have been reported in fast atom bombardment mass spectrometry (FAB-MS),[26] low-energy collision induced dissociation (CID),[27,28] high-energy CID,[29] matrix-assisted laser desorption/ionization (MALDI) photodissociation (PD),[25] and MALDI post-source decay (PSD).[25] Electron transfer dissociation (ETD) and electron capture dissociation (ECD) produce reliable c_n+57 and z_n-57 ions that arise from cleavage between the C_α and the additional carbon incorporated into the backbone of isoAsp residues.[30–36] Additionally, side chain cleavages in the form of *w*-, *d*-, and *v* ions are often only observed for Asp residues and not isoAsp residues.[25,29] ^{18}O-Labeling of deamidation products can provide mass distinction between Asp/isoAsp when paired with reversed phase liquid chromatography.[37,38]

Whereas unique ions characteristic of isoAsp are preferable for identification, differences in relative ion abundances can also provide insight into the identity of the questioned residue. FAB-MS[39] and CID[40] produce less abundant *b*- and *a* ions and more abundant *y* ions at isoAsp residues relative to the same ions observed for Asp, and Asp also tends to form a more intense immonium ions.[41] MALDI free-radical initiated peptide sequencing (FRIPS) provides differences in the abundance of neutral losses—particularly H_2O and CO_2—between Asp and isoAsp, and it generally favors more intense peaks for Asp residues.[25] Also, ETD has been shown to provide more intense *z* ions for isoAsp relative to Asp.[33]

Unique ions and differences in relative ion abundances can both distinguish Asp and isoAsp residues from one another in peptides; however, such diagnostics cannot differentiate L- and D epimers of Asp and isoAsp because the epimers only differ in their stereochemistry and cannot yield unique mass fragments. One method that has shown great potential for chiral differentiation is radical-directed dissociation (RDD).[42–46] RDD is a radical based fragmentation technique that generates a radical through site-specific cleavage of a carbon-iodine bond by photodissociation.[47] Peptides are first modified to include a C–I bond by attaching a chromophore, such as iodobenzoic acid to the N-terminus or by inserting an iodine into an existing tyrosine residue. The peptide is then ionized, isolated in a 2D or 3D ion trap and subjected to a 266 nm pulsed laser to induce photodissociation of the C–I bond and create a radical. The radical product is then subjected to collisional activation to create radical-induced cleavages.[45]

RDD spectra often show significantly different spectra for L- and D epimers of the same peptide sequence, with many peaks having different relative abundances between the two epimers. To quantitate this degree of differentiation, an *R* value can be calculated, which compares the intensity ratio of a pair of peaks in the spectrum of the L-Asp epimer to the same pair of peaks in the spectrum of the D-Asp epimer according to eqn (1).[48] R_A and R_B represent the pair of peaks with the largest difference in abundance between the two epimers.

$$R_{\text{chiral}} = R_A/R_B \quad (1)$$

R values greater than one indicate some degree of differentiation, and larger *R* values indicate a greater degree of confidence in the discrimination. CID typically gives relatively low *R* values for differentiating amino acid epimers, ranging from 1.0–7.0.[45] ETD–CID gives slightly higher *R* values than CID, ranging from 2.0–9.0, while RDD can provide *R* values from 7.0–30.0 for differentiating Asp epimers.[45,49] RDD's ability to generate the largest *R* values has made it the preferred fragmentation method for differentiating L- and D epimers of Asp.

Charge transfer dissociation (CTD) also generates radical species in peptides through interactions of protonated or deprotonated precursors with a beam of kiloelectronvolt helium cations. The fast helium cations effectually abstract an electron from the precursor.[50] CTD is effective at providing numerous backbone cleavages of peptides—including *a*-, *b*-, *c*-, *x*-, *y*-, *z*-, *d*-, *w*- and *v* ions—the last three of which are especially useful side chain losses.[51] The radical-driven nature of fragmentation in CTD implies that it might perform similarly to RDD for the discrimination of L- and D epimers of Asp. Additionally, the numerous fragments produced by CTD could provide distinction between Asp and isoAsp. The current work therefore investigated synthetic versions of peptides derived from crystallin proteins containing isomers of Asp using both CTD and CID to identify discriminatory features of the spectra

that can provide distinction between the different isomeric forms.

Methods

Instrumentation

A Bruker amaZon 3D ion trap mass spectrometer, modified to perform CTD, was used for all experiments. The instrument modifications are described elsewhere.[51] Ultra-high purity (UHP) helium was used as the CTD reagent gas.

Samples

Synthetic versions of crystallin peptides were synthesized following an accelerated FMOC-protected solid-phase peptide synthesis protocol[52] and provided by the Julian Laboratory (University of California Riverside, Riverside, CA). Each peptide was reconstituted in a water/acetonitrile/formic acid mixture (49.5 : 49.5 : 1, v/v/v) with final concentrations between 50–100 μM. The peptides included FVIFLDVK and HFSPEDLTVK, which are found within sheep[42] and human[53] αA crystallin, and GYQYLLEPGDFR, which is common to mouse βB1 crystallin.[54] Each peptide was fabricated in four different versions, with either L-Asp, L-isoAsp, D-Asp, or D-isoAsp as the D residue.

Method

Peptide solutions were ionized by a static nanospray source with a voltage of 1500–1800 V. An isolation width of 4 Da was used during precursor isolation, and the low mass cutoff was set to m/z 250 during CTD. For comparison experiments, CID experiments were performed with a reaction amplitude between 0.5–2.0 V for 50 ms, with Smartfrag disabled. For CTD experiments, the pressure in the vacuum chamber was maintained at ~1.2×10^{-5} mbar, and the ion beam was pulsed on for 100 ms with a voltage of 5–7 kV. The ions gain ~80% of the anode potential so have between 4–5.6 keV of kinetic energy. Product ion spectra were collected for 1–2 minutes in enhanced-resolution mode. After CTD, unreacted precursor ions were removed using resonance ejection at the MS^3 level to minimize space-charge effects and improve the mass accuracy and signal-to-noise ratio.

Data analysis

Spectra were converted to mzML format using MSConvert (http://proteowizard.sourceforge.net/download.html) and worked up in mmass.[55–57] The averaged spectra were normalized to the base peak and automated peak picking was performed using a signal-to-noise threshold of 5.0 and an absolute intensity threshold of 0.3. Fragmentor (https://sites.google.com/ucr.edu/jlab/software/fragmentor?authuser=0) was used to predict the masses of peptide fragments and aid in annotation. Peaks were only labeled if they exceeded the S/N thresholds, were within ±0.2 Da of the theoretical mass, and if the ^{13}C isotope peak met or exceeded the expected abundance relative to the ^{12}C isomer. R values of epimers were calculated using RIsomer (https://sites.google.com/ucr.edu/jlab/software/r-isomer?authuser=0). Single-factor analysis of variance (ANOVA) was performed with SPSS v28 to identify significantly different peaks between isomers and epimers of aspartic acid.

Results & discussion

CTD fragmentation produced numerous types of backbone and side chain cleavages for the peptides studied and provided 100% sequence coverage, in most cases. In addition to the b- and y ions commonly observed with CID, CTD produced a series of a-, x- and z ions and some c ions (Fig. 1). Aligned with previous observations, many of the backbone cleavages were radical species, like the a+1, x+1, and z+1 ions that are typically found in other high energy fragmentation techniques.[50,58] As a generalization, increasing the charge state of the precursor ion from 1+ to 2+ increased the number of observed fragments, and CID produced primarily b- and y ions, as well as neutral losses and a few a ions.

L-Asp *vs.* L-isoAsp

Before comparing the CTD spectra of Asp and isoAsp, we first identified commonly observed isoAsp peaks from other methods of tandem mass spectrometry, as outlined in Table 1. After annotating the CTD spectra of peptides containing either Asp or isoAsp, we compared the fragments obtained through CTD to those observed using other methods. For instance, the b_6 ion in FVIFLDVK was about 80% less intense for the isoAsp version relative to the Asp version. However, there was no meaningful difference in ion abundance of the b_{10} ions for the Asp and isoAsp versions of GYQYLLEPGDFR, and the b_6 ion in HFSPEDLTVK was actually more intense for isoAsp than for Asp, which is in contrast to the trend observed using CID[40] and FAB-MS.[39] As a generalization, CTD produced a ions that are enhanced for Asp residues and y- and z ions that are enhanced for isoAsp residues. For example, the a ions for Asp in $FVIFLDVK^{1+}$ and $GYQYLLEPGDFR^{2+}$ are significantly more intense ($p < 0.05$) than the same ions for isoAsp residues. The a_{10} ion for $GYQYLLEPGDFR^{1+}$ was also observed to be slightly more intense for Asp than isoAsp, but the difference was less significant ($p = 0.114$). These results are similar to those obtained with FAB-MS.[39]

Whereas enhanced a ions in a CTD spectrum can help confirm the presence of Asp residues in a peptide, enhanced z- and y ions are helpful in identifying isoAsp residues. Regardless of the precursor charge state, the z_3 ion for FVIFLDVK was significantly more intense ($p < 0.05$) for the sequence containing isoAsp rather than Asp in the sixth position. Likewise, the z_5 ion was significantly more intense ($p < 0.05$) for isoAsp relative to Asp in $HFSPEDLTVK^{2+}$. These observations are consistent with those of MALDI-FRIPS[25] and ETD.[33] The z_3 ion for GYQYLLEPGDFR was too low in abundance for confident assignment. When observed, y ions were also significantly more intense ($p < 0.05$) for isoAsp relative to Asp in all but one case. In that exception, the y_3 ion was isoba-

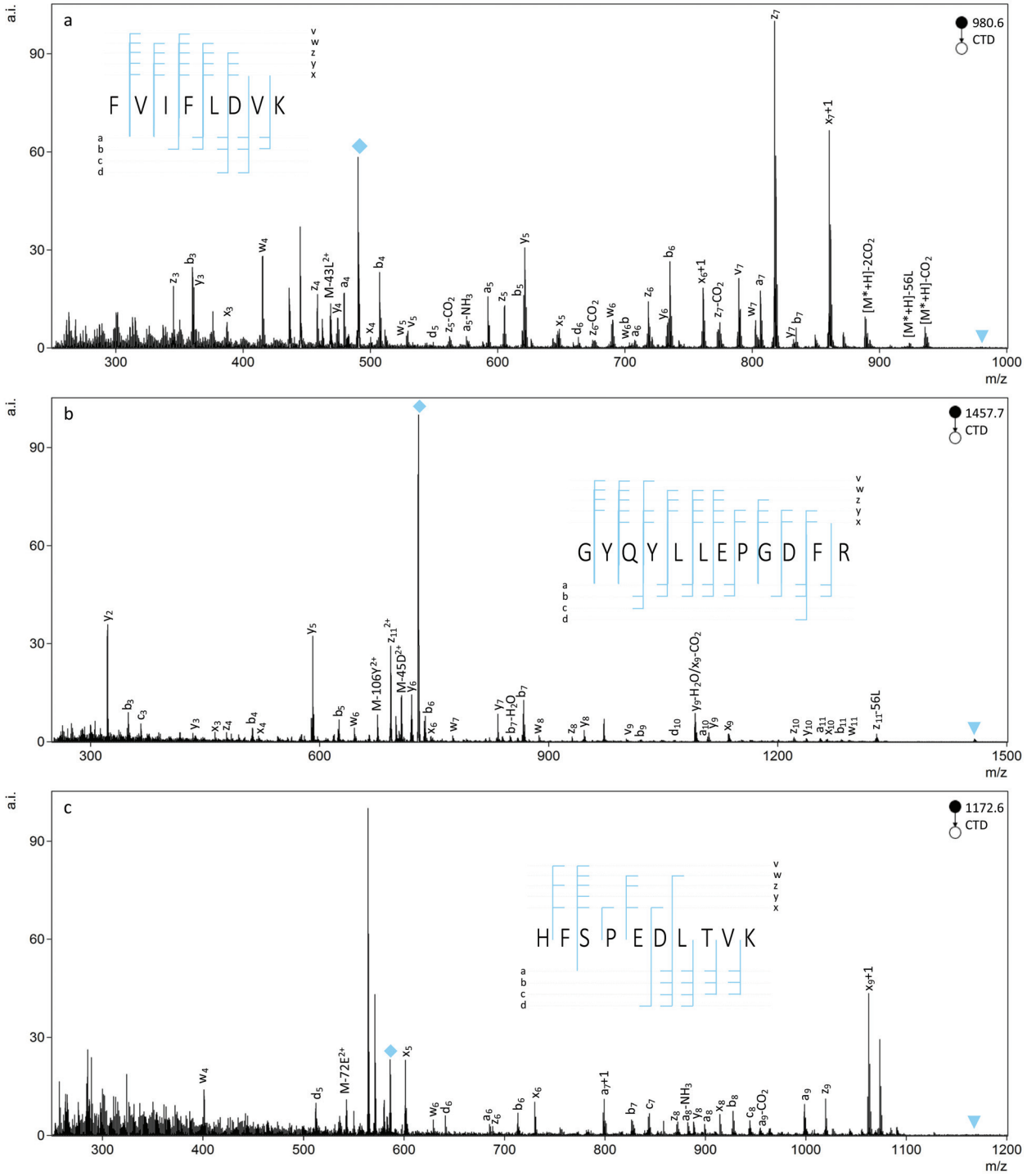

Fig. 1 CTD spectra of all-L peptides: (a) FVIFLDVK (b) GYQYLLEPGDFR and (c) HFSPEDLTVK with inset fragment maps. Triangles represent the resonantly ejected precursor and diamonds represent the CTnoD product ion.

ric with the ^{13}C peak of the b_3 ion of FVIFLDVK at m/z 360.2. The general trends observed for Asp and isoAsp in the various CTD spectra are consistent with those reported for CID[40] and MALDI-PSD.[25]

Table 1 contains a summary of CTD observations and the common isoAsp identifiers reported in the literature and only apply to L-forms of Asp/isoAsp; D-forms of Asp/isoAsp provide a more complicated problem that will be addressed in a different section.

The helpful b_n+H_2O and y_n-46 ions observed in collisionally activated peptides of isoAsp residues were not observed with CTD, but a single c_5+57 ion was observed at m/z 694.4 for

Table 1 Commonly observed isoAsp identifiers relative to Asp among different dissociation methods

isoAsp identifiers	Observed with	CTD observations
Decreased *b* ions	FAB-MS[39] CID[40]	Inconsistent
Decreased *a* ions	FAB-MS[39]	Consistent
Increased *y* ions	CID[40] MALDI-PSD[25]	Inconsistent
Increased *z* ions	MALDI-FRIPS[25] ETD[33]	Consistent
b_n+H_2O, y_n-46	CID[27–29] FAB-MS[26] MALDI-PSD[25] MALDI-PD[25]	Not observed
c_n+57, z_n-57	ECD[30–32] ETD[35,36,59] MALDI-FRIPS[25]	Inconsistent
Decreased -CO_2	MALDI-FRIPS[25]	Not observed

FVIFLDVK^{2+} (Fig. 2). This unique c_n+57 ion for iso-Asp was first observed with ECD, and it has become a reliable diagnostic ion in ECD and ETD to differentiate Asp and isoAsp residues.[32] The cleavage between the C_α and the extra carbon inserted into the peptide backbone of isoAsp results in a fragment at c_n+57 that cannot be produced when an Asp residue is present. Notably, we observe this unique ion present in both the L form and D form of isoAsp in FVIFLDVK, which suggests that the mechanism is not sensitive to chiral differences. The c_5+57 fragment was only observed for this particular peptide, though, so although we demonstrated that CTD is capable of producing this diagnostic ion in one example, the formation of this type of product ion in CTD is not reliably present in all peptides that contain Asp/isoAsp.

L/D Epimers of Asp

To differentiate L- and D epimers of Asp using CTD, we first identified peaks that were significantly different in abundance between the epimers. We also used CID spectra of the same peptides as a benchmark. Significant differences in ion abundances were determined using one-way analysis of variance (ANOVA) using Asp epimerization as the fixed factor. Each test included three replicate measurements of each peptide. To be considered for one-way ANOVA, peaks had to be present with a signal-to-noise (S/N) ratio greater than 5 in at least one spectrum of the two epimers. The number of significant differences and the significance of the differences—as assessed by the significance, p, of the F values—were both considered as metrics for the reliability of epimer discrimination.

Fragmentation of singly charged peptide precursors produced a similar number of peaks that contained significant ($p < 0.05$) abundance differences in both CTD and CID spectra. However, for the doubly charged peptides, CTD produced a greater number of significantly different peaks than CID (Table 2). The identities of the significant peaks indicate a few trends in the types of ions that may be useful for discriminating between L/D forms of Asp. The most promising trend is a potential side chain loss (b_n-45D) from aspartic acid (where

Table 2 Numbers of significantly different peaks for different precursor charge states and dissociation methods for the discrimination of D and L epimers of Asp and isoAsp[a]

Sequence	CTD 1 + precursor	CID 1 + precursor	CTD 2 + precursor	CID 2 + precursor
FVIFL**D**VK	30	25	51	12
FVIFL**Di**VK	24	45	51	13
GYQYLLEPG**D**FR	9	—[b]	40	18
GYQYLLEPG**Di**FR	48	—[b]	50	25
HFSPE**D**LTVK	19	20	83	15
HFSPE**Di**LTVK	19	11	55	20

Significance assessed using one-way ANOVA using D epimer as the fixed factor and $p < 0.05$. [a] The sequences of the peptides are identified by single letter codes with **Di** representing isoaspartic acid. Bold, underlined residues correspond to the site of epimerization. [b] CID data not collected.

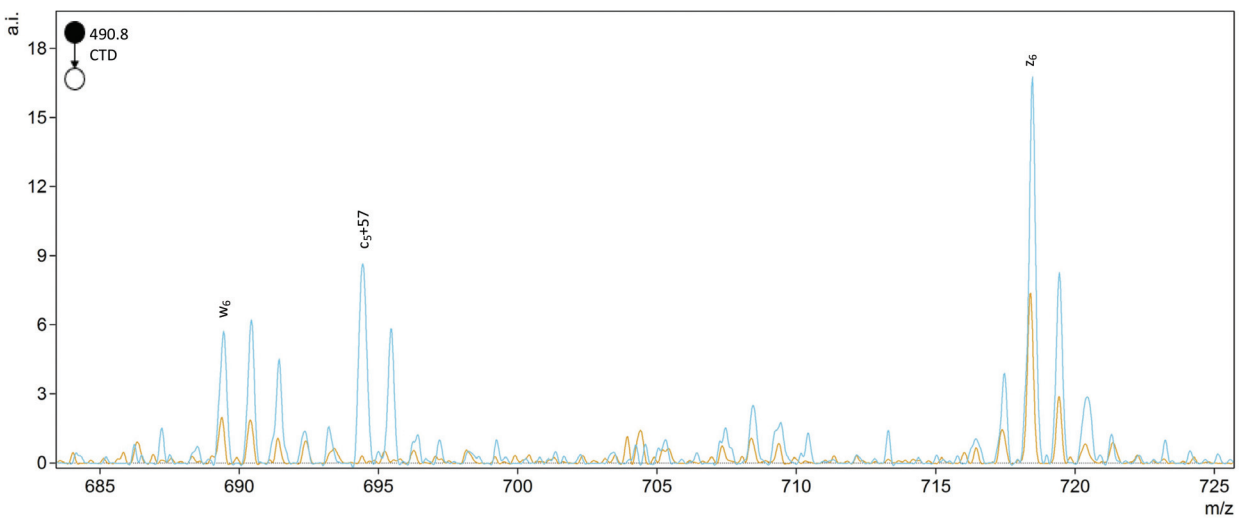

Fig. 2 Comparison of the D epimers of FVIFL**Di**VK (blue) and FVIFL**D**VK (orange). The peak at m/z 694.4 for c_5+57 is unique to the isoAsp residue.

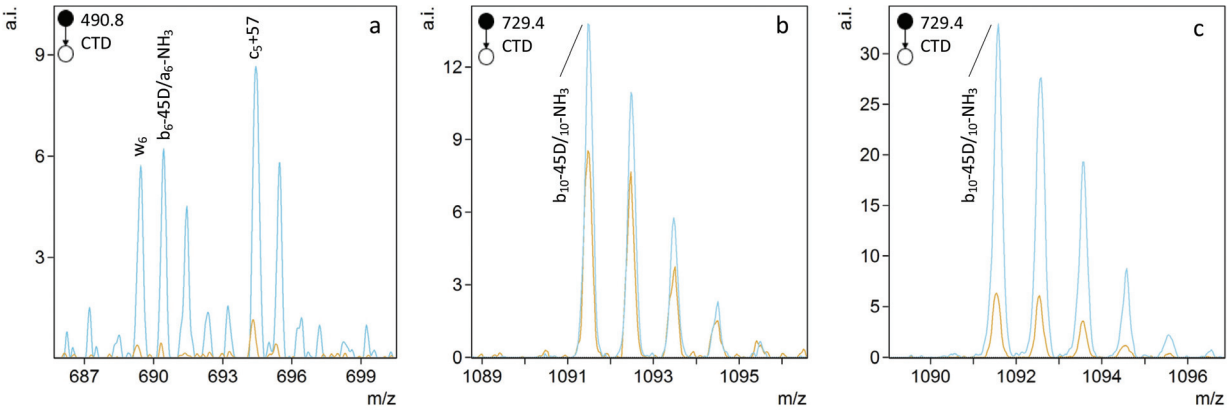

Fig. 3 CTD of L- and D epimers of (a) FVIFLDiVK, (b) GYQYLLEPGDFR, and (c) GYQYLLEPGDiFR showing more intense ions corresponding to b_n-45D/a_n-NH_3 for the D epimer of Asp (blue) relative to the L epimer (orange).

the postscript D indicates the neutral loss is most likely form the aspartic acid residue). When observed, the b_n-45D peak is more intense for the D-epimer (Fig. 3). Unfortunately, without higher mass resolution, we cannot distinguish b_n-45D ions from a_n-NH_3 ions because they are nominal isobars. Whether the ion is the loss of the Asp/isoAsp side chain or a neutral loss of ammonia is less important than the observation that the peak occurs at a greater abundance for one epimer over the other; either way, the peak can still be used to positively identify the D epimer. If the ion is in fact the loss of the aspartic acid side chain, this observation suggests the side chain is more readily lost from the D form relative to the L-form and presumably relates to the re-arrangements that are made possible by the three-dimensional configuration of the peptide.

Other neutral losses from backbone cleavages, like -H_2O and -CO_2, are more abundant for the D epimer than the L epimer in several cases. For example, b_{10}-CO_2 is more abundant for D epimers of GYQYLLEPGDFR and GYQYLLEPGDiFR, whereas an x_5-CO_2 is more abundant for the D epimer of HFSPEDLTVK. Additionally, the z_3-H_2O and z_5-H_2O ions are more abundant for the D epimers of FVIFLDVK and HFSPEDLTVK, respectively. Although not observed in every case, these neutral losses seem to be preferred for the D epimers and thus could be helpful in identifying the chirality of Asp residues.

We also observed significant differences in ion abundances for peaks that are not as obviously related to the proximity of the D residue. For example, the z_4 fragment for FVIFLDVK is significantly more intense for the version containing D-Asp relative to L-Asp, but this cleavage site is one amino acid residue removed from the site of epimerization. Since the epimers differ only in their stereochemistry, these differences in ion abundances using CTD indicate that fragmentation behavior is sufficiently sensitive to conformational changes as to be readily observable at cleavage sites not directly related to the site of epimerization.

To quantify the degree of chiral discrimination possible with CTD, *R* values were calculated for pairs of epimers with

Table 3 Maximum *R* values obtained with CTD and CID for the discrimination of D and L epimers of Asp and isoAsp[a]

	1+ precursor		2+ precursor	
Sequence	CTD	CID	CTD	CID
FVIFLDVK	5.8	18.5[b]	9.3	1.0
FVIFLDiVK	10.2	11.0[b]	16.8	1.0
GYQYLLEPGDFR	1.6	—[c]	2.8	4.1
GYQYLLEPGDiFR	19.9	—[c]	48.2	5.3
HFSPEDLTVK	26.3	1.2	69.8	5.0
HFSPEDiLTVK	41.0	7.9	37.5	2.8

[a] The sequences of the peptides are identified by single letter codes with Di representing isoaspartic acid. Bold, underlined residues correspond to the site of epimerization. [b] The unexpectedly large *R* values present with CID may be attributed to unintentional differences in the accumulation times between two CID spectra during data collection. [c] CID data not collected.

paired peak lists that were already determined to be significantly different between the spectra of the two epimers, as identified through one-way ANOVA. The *R* values shown in Tables 3 and 4 were calculated from the mean of three replicate peak abundances for each peak for each epimer. In some cases, CTD produced one or more unique peaks for one epimer, such as the b_6-45D/a_6-NH_3 peak for FVIFLDVK in Fig. 3, and the a_9-H_2O peak for HFSPEDLTVK in Fig. 4. In these cases, CTD provides unequivocal differentiation between the two epimers. In contrast, CID did not provide any unique peaks for any of the peptides relative to their epimers.

Only ions present in both spectra with S/N greater than 5 were considered for *R* value calculations. In almost every case, CTD produced *R* values that were notably larger than CID. In fact, the *R* values obtained for CTD match or exceed those of RDD, which is the current gold standard and typically delivers *R* values in the range of 2.0–30.0.[45,49]

The identities of the pairs of peaks used to calculate *R* values were also investigated to see if they were obviously related to the altered Asp or isoAsp residues. Epimerization

Table 4 Maximum *R* values and other related peaks for the discrimination of D and L epimers of Asp and isoAsp obtained with CTD and CID for precursor peptides with different charge states.[a] Epimers with unique fragments in CTD were excluded from these calculations

	CTD				CID			
	1+ precursor		2+ precursor		1+ precursor		2+ precursor	
Sequence	*R* value	Related peaks	*R* value	Related peaks	*R* value	Related peaks	*R* value	Related peaks
FVIFL**D**VK	5.8	x_6-H_2O^+ b_5^+	9.3	a_7^+ z_5-58K^{2+}	18.5[b]	Unassigned y_4^+	1.0	
FVIFL**Di**VK	10.2	a_5^+ c_4-15V$^+$	16.8	b_6^+ b_3^+	11.0[b]	M-H_2O^+ Unassigned	1.0	
GYQYLLEPG**D**FR	1.6	M*-45D^{2+} x_2^+	2.8	M-CO_2^{3+} b_3^+	—[c]	—[c]	4.1	y_8^+ Unassigned
GYQYLLEPG**Di**FR	19.9	M-H_2O^{2+} y_6-CO_2^+	48.2	y_9-H_2O y_5^{2+}	—[c]	—[c]	5.3	y_8^+ b_7^+
HFSPE**D**LTVK	26.3	M*-59E-56L$^+$ x_5^+	69.8	y_8-71K x_6+1^+	1.2	b_9^+ y_8^+	5.0	b_6^+ Unassigned
HFSPE**Di**LTVK	41.0	c_6^+ M*-45D-43L$^+$	37.5	z_6^+ a_7^{2+}	7.9[b]	M-H_2O–NH_3^+ Unassigned	2.8	M-H_2O^+ y_4^+

[a] The sequences of the peptides are identified by single letter codes with Di representing isoaspartic acid. Bold, underlined residues correspond to the site of epimerization. [b] The unexpectedly large *R* values present with CID may be attributed to unintentional differences in the accumulation times between two CID spectra during data collection. [c] CID data not collected.

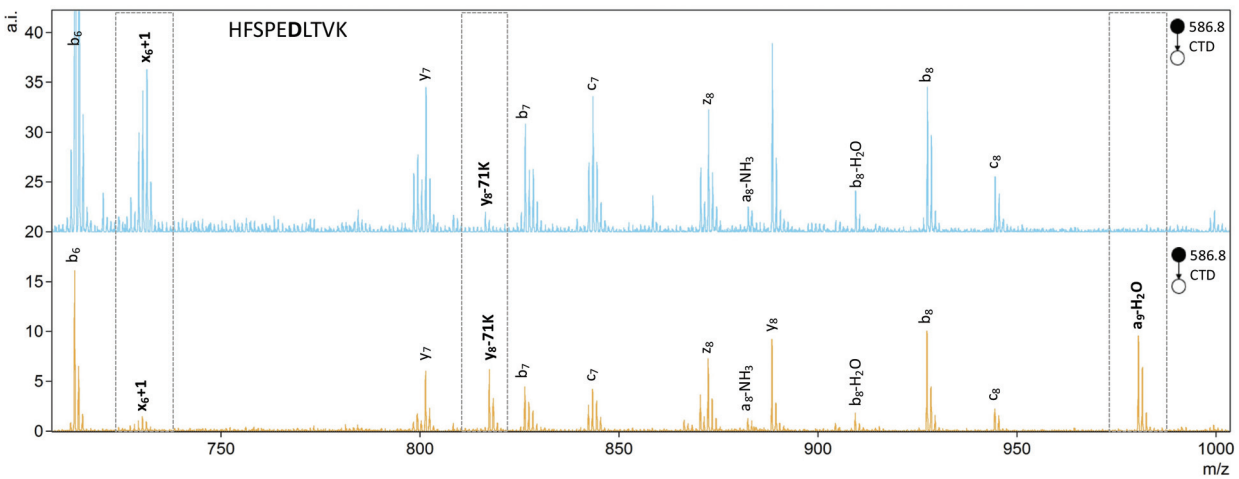

Fig. 4 CTD of L- (orange) and D- (blue) epimers of HFSPE**D**LTVK^{2+} showing the differences in relative peak abundances between spectra. The peaks that vary the most between the two spectra are the y_8-71K ion and the x_6+1 ion, which together give an *R* value = 69.8. Additionally, the a_9+H_2O ion is unique to L-Asp. The peaks of interest are indicated by boxes.

can disturb the three-dimensional structure of the entire peptide, so differences in fragment ion abundances may not always be obviously related to the Asp residue. In fact, with CID, most of the peaks are backbone cleavages or involve neutral losses unrelated to the Asp/isoAsp residue, so there is little, or no, information one can gain about what types of cleavages can be enhanced or hindered with L/D epimers or how differences in fragment ion abundances can be used to provide predictions for new Asp-containing peptides. For CID, there are only two cases in which at least one of the peaks are adjacent to the Asp/isoAsp residues. For the L- and D epimers of HFSPE**D**LTVK, a b_6 ion on the C-terminal side of Asp is significantly different, and for HFSPE**Di**LTVK, a y_4 ion on the C-terminal side of isoAsp is significantly different. For CTD, many of the significant peaks are adjacent to, or one residue removed from, the Asp/isoAsp residue (Table 4).

Herein, CTD demonstrates a high degree of chiral discrimination that is similar to, or greater than, RDD and ETD. Furthermore, D epimers produced more abundant b_n-45D/a_n-NH_3 ions that can provide confidence in assigning the chirality of an Asp residue in an unknown peptide. Though this specific ion is not always observed, the high *R* values obtained with CTD can be used to identify peptides with epimerization present in the sequence. Comparisons with standards of known chirality could then provide additional clarity in identifying the location and type of epimerization, which could be useful in the analysis of peptide mixtures when coupled to LC.

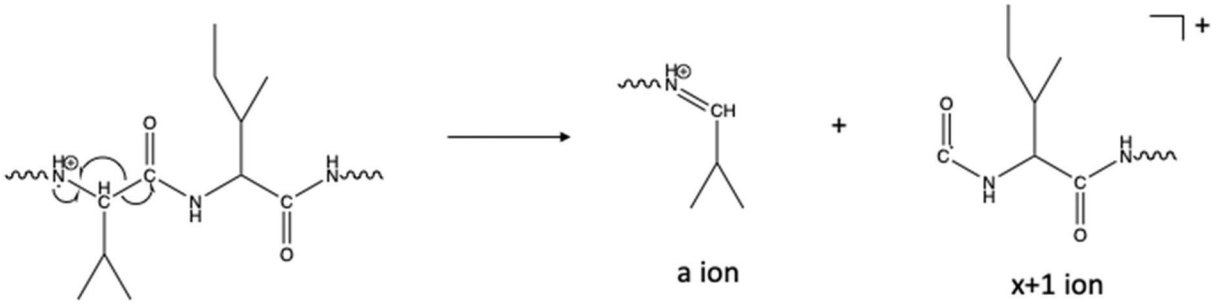

Scheme 1 One proposed pathway for the formation of *a*- and *x*+1 ions.[64] Alternative pathways are also possible.[60,62,63]

a-/*x*-Ion formation

The abundance of a_n+1 radical ions in the CTD spectra are reminiscent of those produced by UVPD,[50] which indicates that the fragmentation mechanism in CTD could follow similar homolytic cleavage of the C_α–C bond to form the a_n+1 ions.[60] In CTD, the homolytic cleavage of the C_α–C bond may be instigated by ionization of the nearby lone pair on the carbonyl oxygen atom, in a similar mechanism to that proposed for metastable atom-activated dissociation (MAD).[61] Among the two isoforms of the three peptides studied, numerous a_n+1 ions were observed in every case. More frequently than the a_n+1 ions, several x_n+1 ions were also observed for each peptide. These findings are consistent with CTD of other low-charge state peptides using CTD.[50]

Among the fragmentation methods capable of producing *a*/*x* ions and their radical counterparts, the a_n+1 ions are most commonly observed. For example, in UVPD, absorption of a 157 nm photon leads to homolytic cleavage to produce a_n+1 and x_n+1 ions. These primary fragments then undergo hydrogen elimination to form the even electron *a*/*x* species.[60,62,63] In addition to the mechanism described above, where CTD fragmentation begins with the radical cation localized on the carbonyl oxygen, the radical could instead be localized on the amide nitrogen, as described by Kjeldsen and coworkers for EDD.[64] As proposed in Scheme 1, α-cleavage of the amide backbone would create an even-electron *a* ion and an x_n+1 ion. Since both a_n+1 and x_n+1 species are observed, it is possible that fragmentation could proceed *via* various competing pathways in CTD. However, given that x_n+1 ions are generally more abundant than a_n+1 ions, excitation of, or radical location on, the amide nitrogen may be preferred in this case. In principle, the x_n+1 ions with a radical on the carbonyl carbon in Scheme 1 could readily form *z*-type ions through the loss of a neutral molecule of isocyanic acid, or CONH.

Conclusions

CTD demonstrates an ability to distinguish isomeric forms of Asp and isoAsp in various peptides on a benchtop instrument without chemical modification of the peptide. For CTD of peptides containing Asp and isoAsp, the increased abundance of *y*- and *z* ions in IsoAsp peptides relative to Asp peptides can be useful in identifying isoAsp residues. In addition, *a* ions tend to be more abundant in Asp-containing peptides relative to IsoAsp. CTD can generate unique c_n+57 ions for isoAsp residues, in a similar fashion to ECD and ETD, and for the L- and D epimers of Asp and isoAsp, CTD demonstrates a degree of chiral discrimination that is similar to, or better than, RDD. Comparison of relative peak abundances in epimer pairs of three Asp-containing peptides and three isoAsp-containing peptides provided *R* values ranging from 2.6–70. Furthermore, a b_n-45D/a_n-NH_3 ion was found to be a reliable indicator for the D isomers of Asp/isoAsp relative to the L isomers. Improved mass resolution would clarify the specific identity of this beneficial fragment, which could then establish its relevance to L/D discrimination of Asp within peptides containing all-L amino acids. These findings show that CTD can provide reliable and structurally meaningful fragments that are sensitive to conformational differences of peptides in the gas phase.

Conflicts of interest

No conflicts of interest to declare.

Acknowledgements

The authors would like to thank Yana A. Lyon for synthesizing the FVIFLDVK peptide used in this study. This work was supported by the National Science Foundation (NSF) (CHE-1710376). The opinions, findings and conclusions or recommendations expressed in this publication are those of the author(s) and do not necessarily reflect the views of NSF.

References

1 N. H. Thayer, C. K. Leverich, M. P. Fitzgibbon, Z. W. Nelson, K. A. Henderson, P. R. Gafken, J. J. Hsu and D. E. Gottschling, *Proc. Natl. Acad. Sci. U. S. A.*, 2014, **111**, 14019–14026.
2 J. N. Savas, B. H. Toyama, T. Xu, J. R. Yates and M. W. Hetzer, *Science*, 2012, **335**, 1–4.

3 E. F. Fornasiero, S. Mandad, H. Wildhagen, M. Alevra, B. Rammner, S. Keihani, F. Opazo, I. Urban, M. S. Sakib, M. K. Fard, K. Kirli, T. P. Centeno, R. O. Vidal, R.-U. Rahman, E. Benito, A. Fischer, S. Dennerlein, P. Rehling, I. Feussner, S. Bonn, M. Simons, H. Urlaub and S. O. Rizzoli, *Nat. Commun.*, 2018, **9**, 1–17.
4 P. A. C. Cloos and S. Christgau, *Matrix Biol.*, 2002, **21**, 39–52.
5 T. L. Spires-Jones and B. T. Hyman, *Neuron*, 2014, **82**, 756–771.
6 S. Forner, D. Baglietto-Vargas, A. C. Martini, L. Trujillo-Estrada and F. M. LaFerla, *Trends Neurosci.*, 2017, **40**, 347–357.
7 T. K. Chaudhuri and S. Paul, *FEBS J.*, 2006, **273**, 1331–1349.
8 W. G. Hodge, J. P. Whitcher and W. Satariano, *Epidemiol. Rev.*, 1995, **17**, 336–346.
9 D. Lam, S. K. Rao, V. Ratra, Y. Liu, P. Mitchell, J. King, M.-J. Tassignon, J. Jonas, C. P. Pang and D. F. Chang, *Nat. Rev. Dis. Primers*, 2015, **1**, 1–15.
10 Y. Tian and B. T. Ruotolo, *Analyst*, 2018, **143**, 2459–2468.
11 Z. Zhang, H. Pan and X. Chen, *Mass Spectrom. Rev.*, 2009, **28**, 147–176.
12 C. R. McCudden and V. B. Kraus, *Clin. Biochem.*, 2006, **39**, 1112–1130.
13 J. L. Bada, *Methods Enzymol.*, 1984, **106**, 98–115.
14 S. Ohtani, Y. Yamada, T. Yamamoto, S. Arany, K. Gonmori and N. Yoshioka, *J. Forensic Sci.*, 2004, **49**, 1–5.
15 N. K. Shah, B. Brodsky, A. Kirkpatrick and J. A. M. Ramshaw, *Biopolymers*, 1999, **49**, 297–302.
16 T. Geiger and S. Clarke, *J. Biol. Chem.*, 1987, **262**, 785–794.
17 X. Zheng, L. Deng, E. S. Baker, Y. M. Ibrahim, V. A. Petyuk and R. D. Smith, *Chem. Commun.*, 2017, **53**, 7913–7916.
18 H. Fukuda, T. Shimizu, M. Nakajima, H. Mori and T. Shirasawa, *Bioorg. Med. Chem. Lett.*, 1999, **9**, 953–956.
19 P. M. Helfman, J. L. Bada and M. Y. Shou, *Gerontology*, 1977, **23**, 419–425.
20 P. M. Masters, J. L. Bada and J. S. Zigler, Jr., *Nature*, 1977, **268**, 71–73.
21 P. M. Masters, J. L. Bada and J. S. Zigler, Jr., *Proc. Natl. Acad. Sci. U. S. A.*, 1978, **75**, 1204–1208.
22 G. H. Fisher, A. D'Aniello, A. Vetere, G. P. Cusano, M. Chávez and L. Petrucelli, *Neurosci. Lett.*, 1992, **143**, 215–218.
23 E. R. Waite, M. J. Collins, S. Ritz-Timme, H. W. Schutz, C. Cattaneo and H. I. M. Borrman, *Forensic Sci. Int.*, 1999, **103**, 113–124.
24 P. P. Hurtado and P. B. O'Connor, *Mass Spectrom. Rev.*, 2012, **31**, 609–625.
25 N. Degraan-Weber, J. Zhang and J. P. Reilly, *J. Am. Soc. Mass Spectrom.*, 2016, **27**, 2041–2053.
26 I. A. Papayannopoulos and K. Biemann, *Pept. Res.*, 1992, **5**, 83–90.
27 P. Schindler, D. Muller, W. Marki, H. Grossenbacher and W. J. Richter, *J. Mass Spectrom.*, 1996, **24**, 967–974.
28 L. J. González, T. Shimizu, Y. Satomi, L. Betancourt, V. Besada, G. Padrón, R. Orlando, T. Shirasawa, Y. Shimonishi and T. Takao, *Rapid Commun. Mass Spectrom.*, 2000, **14**, 2092–2102.
29 S. A. Carr, M. E. Hemling, M. F. Bean and G. D. Roberts, *Anal. Chem.*, 1991, **63**, 2802–2824.
30 J. J. Cournoyer, C. Lin and P. B. O'Connor, *Anal. Chem.*, 2006, **78**, 1264–1271.
31 J. J. Cournoyer, C. Lin, M. J. Bowman and P. B. O'Connor, *J. Am. Soc. Mass Spectrom.*, 2007, **18**, 48–56.
32 J. J. Cournoyer, J. L. Pittman, V. B. Ivleva, E. Fallows, L. Waskell, C. E. Costello and P. B. O'Connor, *Protein Sci.*, 2005, **14**, 452–463.
33 P. B. O'Connor, J. J. Cournoyer, S. J. Pitteri, P. A. Chrisman and S. A. McLuckey, *J. Am. Soc. Mass Spectrom.*, 2006, **17**, 15–19.
34 N. P. Sargaeva, C. Lin and P. B. O'Connor, *J. Am. Soc. Mass Spectrom.*, 2011, **22**, 480–491.
35 N. P. Sargaeva, C. Lin and P. B. O'Connor, *Anal. Chem.*, 2011, **83**, 6675–6682.
36 W. Y. K. Chan, T. W. D. Chan and P. B. O'Connor, *J. Am. Soc. Mass Spectrom.*, 2010, **21**, 1012–1015.
37 S. Wang and I. A. Kaltashov, *Anal. Chem.*, 2013, **85**, 6446–6452.
38 M. Liu, J. Cheetham, N. Cauchon, J. Ostovic, W. Ni, D. Ren and Z. S. Zhou, *Anal. Chem.*, 2012, **84**, 1056–1062.
39 J. R. Lloyd, M. L. Cotter, D. Ohori and D. L. Doyle, *Biomed. Environ. Mass Spectrom.*, 1988, **15**, 399–402.
40 W. D. Lehmann, A. Schlosser, G. Erben, R. Pipkorn, D. Bossemeyer and V. Kinzel, *Protein Sci.*, 2000, **9**, 2260–2268.
41 A. Schlosser and W. D. Lehmann, *J. Mass Spectrom.*, 2000, **35**, 1382–1390.
42 Y. A. Lyon, G. M. Sabbah and R. R. Julian, *J. Proteome Res.*, 2017, **16**, 1797–1805.
43 Y. Tao and R. R. Julian, *Anal. Chem.*, 2014, **86**, 9733–9741.
44 T. Ly and R. R. Julian, *J. Am. Chem. Soc.*, 2008, **130**, 351–358.
45 Y. Tao, N. R. Quebbemann and R. R. Julian, *Anal. Chem.*, 2012, **84**, 6814–6820.
46 L. Zhang and J. P. Reilly, *J. Am. Soc. Mass Spectrom.*, 2009, **20**, 1378–1390.
47 T. Ly, X. Zhang, Q. Sun, B. Moore, Y. Tao and R. R. Julian, *Chem. Commun.*, 2011, **47**, 2835–2837.
48 W. A. Tao, D. Zhang, E. N. Nikolaev and R. G. Cooks, *J. Am. Chem. Soc.*, 2000, **122**, 10598–10609.
49 Y. A. Lyon, G. Beran and R. R. Julian, *J. Am. Soc. Mass Spectrom.*, 2017, **28**, 1365–1373.
50 W. D. Hoffmann and G. P. Jackson, *J. Am. Soc. Mass Spectrom.*, 2014, **25**, 1939–1943.
51 P. Li and G. P. Jackson, *J. Am. Soc. Mass Spectrom.*, 2017, **28**, 1271–1281.
52 C. Hood, G. Fuentes, H. Patel, K. Page, M. Menakuru and J. H. Park, *J. Pept. Sci.*, 2008, **14**, 97–101.
53 Y. A. Lyon, G. M. Sabbah and R. R. Julian, *Exp. Eye Res.*, 2018, **171**, 131–141.
54 X. Liu, M. Zhang, Y. Liu, P. Challa, P. Gonzalez and Y. Liu, *Mol. Vision*, 2008, **14**, 2404–2412.

55 M. Strohalm, M. Hassman, B. Košata and M. Kodíček, *Rapid Commun. Mass Spectrom.*, 2008, **22**, 905–908.
56 M. Strohalm, D. Kavan, P. Novák, M. Volný and V. Havlíček, *Anal. Chem.*, 2010, **82**, 4648–4651.
57 T. H. J. Niedermeyer and M. Strohalm, *PLoS One*, 2012, **7**, e44913.
58 P. Li, I. Kreft and G. P. Jackson, *J. Am. Soc. Mass Spectrom.*, 2017, **29**, 284–296.
59 N. P. Sargaeva, C. Lin and P. B. O'Connor, *Anal. Chem.*, 2009, **81**, 9778–9786.
60 W. Cui, M. S. Thompson and J. P. Reilly, *J. Am. Soc. Mass Spectrom.*, 2005, **16**, 1384–1398.
61 S. L. Cook, O. L. Collin and G. P. Jackson, *J. Mass Spectrom.*, 2009, **44**, 1211–1223.
62 L. Zhang and J. P. Reilly, *Anal. Chem.*, 2009, **81**, 7829–7838.
63 L. Zhang, W. Cui, M. S. Thompson and J. P. Reilly, *J. Am. Soc. Mass Spectrom.*, 2006, **17**, 1315–1321.
64 F. Kjeldsen, O. A. Silivra, I. A. Ivonin, K. F. Haselmann, M. Gorshkov and R. A. Zubarev, *Chem. – Eur. J.*, 2005, **11**, 1803–1812.